Bioresource Technology 102 (2011) 1019–1027

Contents lists available at ScienceDirect

Bioresource Technology

journal homepage: www.elsevier.com/locate/biortech

Post-anoxic denitrification driven by PHA and glycogen within enhanced biological phosphorus removal

Erik R. Coats [a,*], Alexander Mockos [a], Frank J. Loge [b]

[a] Department of Civil Engineering, University of Idaho, PO Box 441022, Moscow, ID 83844-1022, USA
[b] Department of Civil and Environmental Engineering, University of California Davis, 1 Shields Avenue, Davis, CA 95616, USA

ARTICLE INFO

Article history:
Received 30 July 2010
Received in revised form 24 September 2010
Accepted 28 September 2010
Available online 20 October 2010

Keywords:
Enhanced biological phosphorus removal
Post-anoxic denitrification
Glycogen
Polyhydroxyalkanoate

ABSTRACT

The objective of this research was to interrogate and develop a better understanding for a process to achieve post-anoxic denitrification without exogenous carbon augmentation within enhanced biological phosphorus removal (EBPR). Sequencing batch reactors fed real wastewater and seeded with mixed microbial consortia were operated under variable anaerobic–aerobic–anoxic and organic carbon loading conditions. The process consistently achieved phosphorus and nitrogen removal, while the observed specific denitrification rates were markedly higher than expected for post-anoxic systems operated without exogenous organic carbon addition. Investigations revealed that post-anoxic denitrification was predominantly driven by glycogen, an intracellular carbon storage polymer associated with EBPR; moreover, glycogen reserves can be significantly depleted post-anoxically without compromising EBPR. Success of the proposed process is predicated on providing sufficient organic acids in the influent wastewater, such that residual nitrate carried over from the post-anoxic period is reduced and polyhydroxyalkanoate (PHA) synthesis occurs.

1. Introduction

Conventional denitrification practices require either mixing of nitrate-rich wastewater with influent raw wastewater (pre-anoxic denitrification) or providing an external carbon source in an anoxic basin downstream of the nitrifying aerobic reactors (post-anoxic denitrification) (Grady et al., 1999). Pre-anoxic operations can potentially yield high specific denitrification rates (SDNRs), given the supply of readily biodegradable carbon, and can further reduce wastewater treatment plant (WWTP) energy demands in that the biochemical oxygen demand (BOD) can be lowered significantly without aeration (Tchobanoglous et al., 2003). Disadvantages include the operating costs associated with delivering high mixed liquor recycle (MLR) flows from the aerobic to anoxic zones; oxygen in the MLR upsetting the process; high MLR diluting the raw wastewater and reducing the SDNR; and incomplete nitrogen removal (Tchobanoglous et al., 2003). While a conventional post-anoxic system eliminates the need for MLR and can yield better overall nitrate removal, additional operational costs are incurred associated with exogenous carbon addition (methanol or acetate (Tchobanoglous et al., 2003)). The non-optimized addition of organic carbon can also increase effluent BOD, and the reducing equivalents gained through pre-anoxic BOD removal are not realized. Microbial endogenous decay can potentially drive post-anoxic denitrification (Vocks et al., 2005), but mode of operation is considered unreliable (Tchobanoglous et al., 2003).

Organic carbon is the critical element to achieve successful denitrification. In this regard, when phosphorus removal requirements are integrated into the wastewater treatment equation, new opportunities for enhanced process efficiencies arise. Specifically, enhanced biological phosphorus removal (EBPR) theory links the cycling of two intracellular organic carbon storage polymers (polyhydroxyalkanoates (PHAs) and glycogen) to phosphorus removal (Fuhs and Chen, 1975; Smolders et al., 1994a,b). Under anaerobic conditions, organic acids present in the wastewater are stored intracellularly by microbes as PHA, with glycogen reserves in part providing necessary metabolic reducing equivalents for PHA synthesis (Arun et al., 1988; Hesselmann et al., 2000; Lemos et al., 2003; Satoh et al., 1992). In the subsequent aerobic environment, PHA is used to restore glycogen reserves and also to fuel microbial growth and phosphorus removal (Maurer et al., 1997; Pereira et al., 1996). In addition to supporting EBPR, PHA and/or glycogen could potentially drive denitrification. Regarding a pre-anoxic EBPR configuration, Activated Sludge Model 2d (Henze et al., 1999) was specifically developed to account for a sub-population of aerobic phosphate accumulating organisms (PAOs) capable of accomplishing denitrification on PHA (population referred to as denitrifying PAOs (DNPAOs)). In this process configuration, anaerobically stored PHA is used both to reduce nitrate and anoxically restore cellular glycogen (Kuba et al., 1996). In contrast, post-anoxic denitrification could potentially be driven by both PHA

* Corresponding author. Tel.: +1 208 885 7559; fax: +1 208 885 6608.
E-mail address: ecoats@uidaho.edu (E.R. Coats).

0960-8524/$ - see front matter © 2010 Elsevier Ltd. All rights reserved.
doi:10.1016/j.biortech.2010.09.104

and glycogen. Such a configuration would eliminate the need for external carbon augmentation and also potentially improve overall total nitrogen removal. Use of the organic carbon present in the influent wastewater would also be maximized to drive both phosphorus and nitrate removal.

The purpose of the research presented and discussed herein was to interrogate the potential to achieve post-anoxic denitrification within EBPR without exogenous carbon addition. Specific objectives of this research were to: (i) determine process operational requirements to achieve post-anoxic denitrification and EBPR, (ii) quantify the range of SDNRs that could be realized for this post-anoxic process, (iii) confirm the source(s) of carbon driving denitrification, and (iv) evaluate the performance of post-anoxic EBPR in terms of both phosphorus and nitrogen removal under variable loading conditions (i.e., mimicking full-scale WWTP operations). Central to this research was the use of real wastewater and mixed microbial consortia, such that results could more readily be transferable to full-scale facilities.

2. Methods

2.1. Source of microorganisms and wastewater

The microbial inoculum and raw wastewater were obtained from the Moscow, ID EBPR WWTP. VFA-rich fermenter liquor was recovered from a bench-top fermenter fed thickened primary solids from the Pullman, WA WWTP; the microbial inoculum for the fermenter was obtained from Pullman's anaerobic digester. Moscow operates a hybrid A^2/O-oxidation ditch process, while Pullman operates a conventional MLE process with a high rate, completely mixed, mesophilic anaerobic digester (Tchobanoglous et al., 2003).

2.2. Bioreactor operating conditions

Four independent sequencing batch reactors (SBRs) were operated, each with an operating volume of 1200 mL. Each SBR (Table 1) was operated under cyclical anaerobic–aerobic–anoxic conditions. All reactors, with exception of reactor B, were augmented with fermenter liquor, and all SBRs were operated on four 6-h cycles a day. SBR operation consisted of four sequential steps: (1) fill, (2) react, (3) settle, and (4) decant. During the fill period, wastewater was added to the reactor, while anaerobic, aerobic, and anoxic conditions were imposed during the react period to facilitate wastewater treatment. Anaerobic conditions were created by diffusing nitrogen gas into each bioreactor. Air was diffused through the reactor to maintain a DO level greater than 2 mg L^{-1} during the aerobic period. Following treatment, biomass was allowed to settle to the bottom of the tank, whereupon treated effluent was withdrawn. Reactors were mixed except during the settle and decant periods. For each operational cycle, the settling period was followed by a two minute decant period and an eight minute feed period. To maintain the target hydraulic residence time (HRT) of 18 h, 400 mL of treated effluent was decanted each cycle, followed by the addition of substrate. Decanting and feeding was accomplished with Watson-Marlow peristaltic pumps (Wilmington, MA, USA). Bioreactor operations were controlled with digital timers. The solids residence time (SRT) was maintained at 20 days, and was controlled by wasting mixed liquor at the end of an aerobic period once a day. Fermenter liquor was produced in a 12-L completely mixed primary solids fermenter, operated as a SBR, with an SRT of 4 days and a HRT of 4 days. The daily decant was centrifuged at approximately 10,000 rpm, with the supernatant (i.e., fermenter liquor) recovered and stored at 4 °C. All reactors operated for this research were maintained at room temperature (approximately 21 °C).

2.3. Analytical techniques

Samples were collected to measure the following parameters: soluble reactive phosphate (P), nitrate-N (NO_3-N), total mixed-liquor suspended solids (MLSS), mixed liquor volatile suspended solids (MLVSS), dissolved oxygen (DO), and ammonia-N (NH_3-N). For soluble constituents, samples were centrifuged, with the supernatant then filtered through a 0.22 μm syringe filter (Millipore Corp., Billerica, MA, USA) prior to testing. P was determined in accordance with Hach (Loveland, CO, USA) method 8048 (equivalent to Standard Methods 4500-PE; (Clesceri LS and Eaton, 1998)). NO_3-N was determined in accordance with Hach method 10020. A Spectronic® 20 Genesys™ spectrophotometer (Thermo Scientific Corp, Waltham, MA, USA) was utilized to measure the absorbance of the reacted sample at a wavelength of 890 nm for P and 410 nm for NO_3-N. Phosphorus and NO_3-N concentrations were determined utilizing a standard curve ($R^2 > 0.99$). MLSS and MLVSS were measured in accordance with Standard Methods 2540 D and 2540 E. DO measurements were collected using a Hach HQ30d Meter with a LDO101 DO Probe. NH_3-N was measured in accordance with Standard Methods 4500-NH_3-D. An Accumet XL60 meter with a Thermo 9512 Ammonia probe was utilized for NH_3-N measurement.

Organic acid concentrations were measured using a Hewlett–Packard (Palo Alto, CA, USA) 6890 Series Gas Chromatograph with a flame-ionization detector (FID). The temperature of the column (Grace Davison Discovery Sciences, Deerfield, IL, USA, Alltech® Heliflex® AT™-Wax Column, length 30 m, internal diameter 0.32 mm) was held constant at 150 °C; the injector was maintained at 210 °C and the detector was operated at 210 °C. Helium was used as the carrier gas at a flow rate of 1.2 mL min^{-1}. Samples were acidified to a pH of 2 with HCl prior to injection. 0.5 μL of sample was injected in 20:1 split mode for analysis. The respective sample organic acid concentrations were confirmed by retention time matching with known standards (acetate, propionate, butyrate, valerate; Grace Davison Discovery Sciences) and quantified using standard curves ($R^2 > 0.99$).

Table 1
Operational characteristics (SRT, HRT, form of substrate; length of anaerobic, aerobic, and post-anoxic periods) of reactors A–D. For the "substrate", 100% raw wastewater indicates that the reactor only received raw wastewater, obtained from the Moscow, ID WWTP. For those reactors that also received fermenter liquor (derived from a lab-scale primary solids fermenter, with primary solids obtained from the Pullman, WA WWTP), the ratio was 90% raw wastewater and 10% primary solids fermenter liquor (v:v).

Reactor	Substrate	SRT (days)	HRT (h)	Anaerobic time (h)	Aerobic time (h)	Anoxic time (h)
A	90% Raw wastewater, 10% Fermenter liquor	20	18	1	2.5	2
B	90% Raw wastewater, 10% Fermenter liquor	20	18	1	1.5	3
C	100% Raw wastewater	20	18	1	2.5	2
D	90% Raw wastewater, 10% Fermenter liquor, augmented with propionate and acetate	20	18	1	2.5	2
D-1 (single run)	90% Raw wastewater, 10% Fermenter liquor, augmented with propionate and acetate	20	18	–	1.5	3
D-2 (single run)	90% Raw wastewater, 10% Fermenter liquor, augmented with propionate and acetate	20	18	–	–	5

Biomass PHA content was determined by gas chromatography/mass spectrometry (GC–MS) (Braunegg et al., 1978). Briefly, dried PHA-rich biomass samples were digested at 100 °C in 2 mL each of acidified methanol (3% v/v sulfuric acid) and chloroform. Benzoic acid was added to the chloroform as an internal standard. Following vortexing of the mixture with 1-mL deionized water, PHA-rich chloroform was recovered for analysis. The chloroform phase was dehydrated by filtering the PHA-rich solution through sodium sulfate prior to analysis. GC–MS was performed on a Thermofinnigan PolarisQ iontrap GC–MS instrument (Thermo Electron Corporation). The sample was introduced using split injection. Separation was achieved on a ZB1 (15 m, 0.25 mm ID) capillary column (Phenomenex, Torrance, California, USA) with helium as the carrier gas (1.2 mL min^{-1}) and an initial temperature of 40 °C (2 min) ramped to 200 °C at 5 °C min^{-1}. The compounds were confirmed by retention time and mass spectral matching with known PHA standards (PHB and PHB-co-HV: Sigma Aldrich; NaHB: Alfa Aeser) as methyl ester derivatives, and quantified based on the internal standard. The Xcalibur software program (Thermo Electron Corporation) was used to facilitate PHA quantitation, and the optimal molecular weight for PHA quantification was determined to be 103 g mol^{-1}. PHB was found to elute at approximately 5.43–5.64 min, while PHV was observed to elute at approximately 8.04–8.37 min; no other forms of PHA were observed. The benzoic acid internal standard eluted at approximately 11.95–12.0 min. Total cellular PHA content was determined on a percent dry weight cell basis (e.g., mass PHA per mass of biomass (MLSS), w/w). Intracellular glycogen was determined according to Parrou and Francois (1997) via digestion and hydrolysis to glucose. Glucose was analyzed enzymatically (Sigma–Aldrich PGO enzyme kit, Saint Louis, Missouri, USA). Sample absorbance was measured at 425 nm using a Spectronic® 20 Genesys™ spectrophotometer.

3. Results and discussion

3.1. Effectiveness of post-anoxic configured EBPR

PHA and glycogen could be biodegraded post-anoxically to drive nitrate reduction within a post-anoxic configured system. Vocks et al. (2005) suggested that glycogen could potentially drive post-anoxic denitrification in an EBPR system, however, their results were based on a single-run batch test, and they acknowledged that cycling of both PHA and glycogen in a continuously operated process needed to be further assessed to understand potential effects on EBPR. Of principle concern is that glycogen reserves, which are critical to drive necessary EBPR metabolisms (Smolders et al., 1994a,b), would be depleted post-anoxically and thus impair EBPR performance.

To assess the potential stability and performance of a post-anoxic EBPR system, we operated a SBR (Reactor A) in the prerequisite cyclical anaerobic–aerobic–anoxic mode for a period of 105 days and fed 90% wastewater and 10% fermenter liquor (v/v) (Table 1). The fermenter liquor-raw wastewater mixture (10%:90%, v/v) organic acid concentration varied from 140–180 mg L^{-1}, with acetic acid being the predominant form (60–65%); other forms of organic acids detected (order of highest to lowest concentration) were propionate (25–30%), butyrate (8–10%), and valerate (<3%). Comparatively, the raw wastewater organic acid concentrations were dominated by acetate and propionate, with minimal butyrate and valerate; total VFA concentrations were 44–55 mg L^{-1}. The wastewater mixture ammonia–nitrogen and phosphorus concentration ranged from 25–45 mg NH_3-N L^{-1} to 20–25 mg P L^{-1}, while the raw wastewater exhibited concentrations of 20–25 mg NH_3-N L^{-1} and 4–6 mg P L^{-1}, respectively. No nitrate was detected. This magnitude of fermenter liquor augmentation yielded VFA, phosphorus, and ammonia concentrations at the beginning of the operational cycle comparable to that observed at full-scale EBPR WWTPs (Neethling et al., 2005). First considering phosphorus removal, as shown (Fig. 1A), the cycling patterns were consistent with EBPR theory, with anaerobic phosphorus release followed by aerobic phosphorus uptake. Near-complete phosphorus removal was realized during the aerobic period. Overall, this steady-state reactor consistently achieved greater than 96% P removal, with concentrations below 0.14 mg P L^{-1} and as low as 0.05 mg P L^{-1}; these effluent values are consistent with EBPR systems augmented with VFAs (Oehmen et al., 2007). No additional P removal occurred post-anoxically; as shown (Fig. 1C), PHA was effectively depleted at the end of the aerobic period. As would be predicted, ammonia was oxidized to nitrate in the aerobic phase, while nitrate was reduced to nitrogen gas in both the post-anoxic and anaerobic phases (Fig. 1B). Although residual nitrate was carried over to the subsequent cycle's anaerobic phase, these results clearly demonstrate that this occurred without compromising the EBPR process. Overall, influent ammonia–nitrogen concentrations were reduced by over 97%, and total effluent ammonia + nitrate concentrations ranged from 8.8 to 12.1 mg L^{-1}.

Anaerobic VFA utilization was in accordance with current EBPR theory, as were PHA and glycogen cycling patterns (Fig. 1C) (Smolders et al., 1994a,b). The quantity of glycogen oxidized anaerobically to provide reducing equivalents for PHA synthesis ranged from 0.44–0.58 C mmol per C mmol PHA. While these values are both higher than observed by others for PAO-dominated EBPR systems (0.28–0.36 per Zhang et al. (2008) and Filipe et al. (2001a)) and as would be predicted by EBPR theory (0.385 per Smolders et al. (1994a)), ratios within or above this range have been measured for successful EBPR systems (Carvalho et al. (2007), Arun et al. (1988)). Excess glycogen utilization (without PHA synthesis) has been linked to the metabolism of glycogen accumulating organisms (GAOs) (Filipe et al., 2001b), the presence of which can impair EBPR. However, given the overall stable reactor performance and other indicators, it would appear that PAOs dominated the consortium.

The ratio of anaerobic phosphorus released-to-gross anaerobic VFA removed (referred to as the P:C ratio) was approximately 0.39–0.60 P-mmol:C-mmol (Table 2). According to Oehmen et al. (2007) and Lopez-Vazquez et al. (2007) this would suggest that the microbial consortium was dominated by PAOs. Further, considering that no secondary phosphorus release occurred in the post-anoxic period, the PAO population would appear to have been dominated by denitrifying PAOs (DNPAOs) (Barnard and Fothergill, 1998). In addition to the P:C being consistent with that expected of EBPR, the influent VFA-to-phosphorus ratio (mg VFA (as COD) per mg P), measured at 25.6–40.8 (Table 2), was also similar to that observed and/or predicted for successful EBPR (Filipe et al., 2001a; Horgan et al., 2010; Smolders et al., 1994a).

Regarding post-anoxic denitrification, it was hypothesized that nitrate removal was driven by either biomass decay or use of PHA and/or glycogen. In regard to cell decay, no measurable reduction in MLVSS was observed during the anoxic phase, although MLVSS measurements are not incontrovertible evidence that endogenous decay was inconsequential to denitrification. An inspection of the specific denitrification rates (SDNRs) does, however, point to the metabolic use of a more readily biodegradable carbon source. The post-anoxic SDNRs exhibited by the consortium ranged from 0.69 to 0.90 mg NO_3 (hr-g MLVSS)$^{-1}$ (Table 3). These SDNRs were higher than expected for systems operated post-anoxically without addition of an exogenous carbon source (0.2–0.6 mg NO_3 (hr-g MLVSS)$^{-1}$ (Grady et al., 1999; Kujawa and Klapwijk, 1999)). In regard to intracellular carbon polymers, it is unlikely that PHA was driving denitrification. First, as noted and shown, PHA was

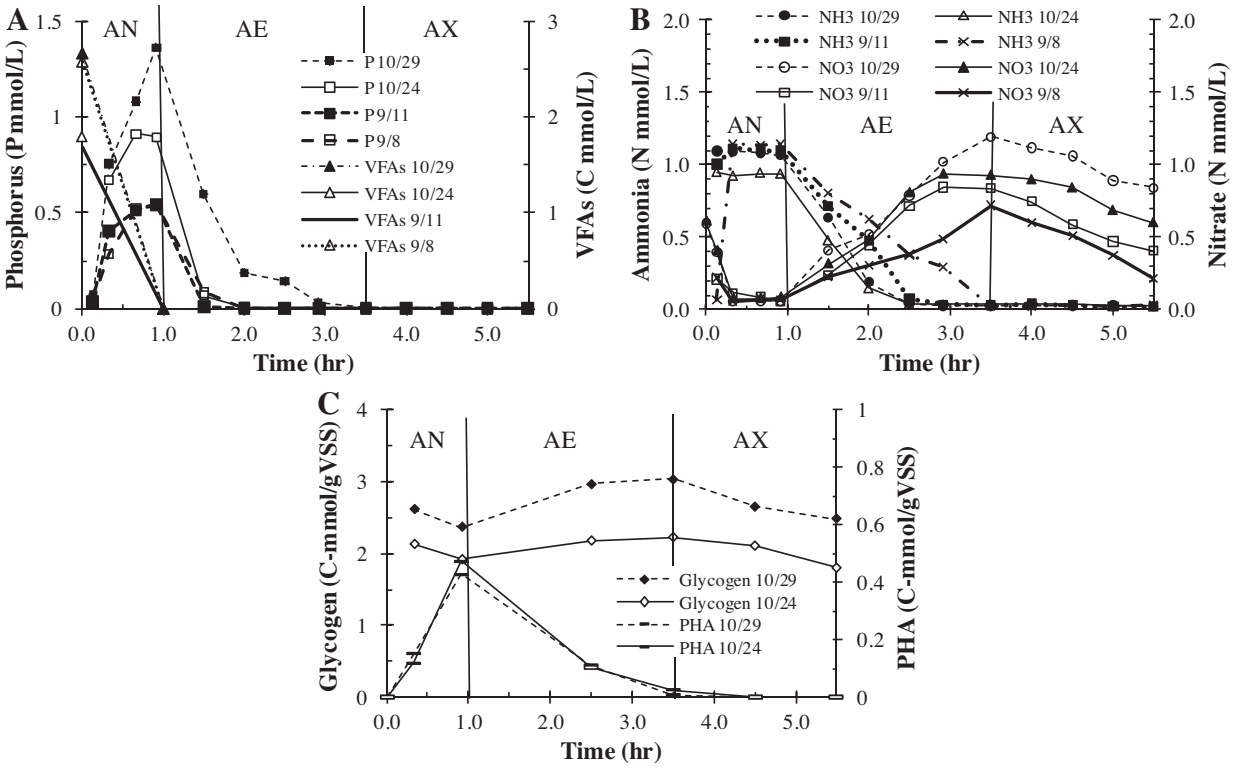

Fig. 1. Performance summary from steady state enhanced biological phosphorus removal reactor (reactor A) operated as a sequencing batch reactor and in post-anoxic mode. Reactor A was operated at a solids retention time of 20 days and a hydraulic residence time of 18 h. (A) Phosphorus and VFAs profiles in reactor A over four operational cycles. Note that VFA measurements were always determined to be fully depleted at the end of the anaerobic period. (B) Ammonia-N and Nitrate-N profiles in reactor A over four operational cycles. (C) Glycogen and PHA profiles in reactor A over two operational cycles.

Table 2
Food-to-microbe, influent VFA-influent phosphorus, and influent VFA-influent ammonia–nitrogen ratios for reactors A–D.

		Reactor A	Reactor B	Reactor C	Reactor D
Food:Microbe ratio	mg VFA (as COD)/g VSS	16.6–43.5	30.5	10.6	52.5
	C mmol VFA/g VSS	0.4–1.3	0.9	0.3	1.6
Influent VFA:P ratio	mg VFA (as COD)/mg P	25.6–40.8	20.4	15.3	54.8
P released:VFA uptaken	P mmol:C mmol	0.39–0.60	0.61	0.04	0.33–0.36
Influent VFA:N ratio	mg VFA/mg NH_4-N	4.1–6.6	5.4	3.16	14.5

Table 3
Details on nitrate-nitrogen stoichiometry and kinetics during the pre-anoxic/anaerobic and post-anoxic periods for reactors A, B, and D.

Reactor operational period	Parameter	Units	Reactor A				Reactor B	Reactor D
			9.8	9.11	10.24	10.29		
Pre-anoxic/anaerobic	NO_3-N reduced	mg/L	2.13	1.74	4.65	4.76	4.29	3.28
		mg/gVSS	0.63	0.50	1.84	2.26	2.86	1.46
	Denitrification rate, r_D	mg NO_3/L-h	7.11	2.74	15.5	15.9	14.3	10.9
	Specific rate of denitrification, SDNR	mg NO_3/gVSS-h	2.09	0.79	6.1	7.5	9.5	4.9
Post-anoxic	NO_3-N reduced	mg/L	5.39	4.78	4.16	3.89	2.38	6.12
		mg/gVSS	1.58	1.38	1.64	1.85	1.58	2.73
	Denitrification rate, r_D	mg NO_3/L-h	2.70	2.39	2.08	1.95	0.79	3.06
	Specific rate of denitrification, SDNR	mg NO_3/gVSS-h	0.79	0.69	0.8	0.9	0.53	1.36
Entire cycle	Nitrate reduced	mg/L	7.52	6.52	8.81	8.65	6.67	9.40

effectively depleted within the aerobic phase (Fig. 1C). Second, the SDNRs were lower than observed for an EBPR system operated in a cyclical anaerobic–anoxic mode (where PHA drove nitrate reduction), which ranged from 1.12 to 10.8 mg NO_3 (hr-g MLVSS)$^{-1}$ (Carvalho et al., 2007), and also for non-EBPR systems wherein PHA was driving denitrification (SDNRs ranging from 1.2 to 2.9 mg NO_3 (hr-g MLVSS)$^{-1}$ (Qin et al., 2005; Third et al., 2003)). However, glycogen reserves usage occurred post-anoxically; it was thus assumed to be the carbon source for denitrification.

3.2. Effects of an extended post-anoxic period

Performance of the post-anoxic configured EBPR Reactor A confirmed process potential. However, considering that the

intracellular glycogen levels were not depleted in the Reactor A post-anoxic period (Fig. 1C), we hypothesized that there was additional denitrification capacity to be gained with a longer post-anoxic period (and commensurately shorter aerobic period). To assess the potential to enhance denitrification, a new SBR (Reactor B; operated for 70 days) was established with a shorter aerobic cycle time and a commensurately longer anoxic cycle time (Table 1). Consistent with Reactor A, the consortium received 90% raw wastewater and 10% fermenter liquor (v/v).

Similar to that observed in Reactor A, the consortium in Reactor B performed well overall in removing phosphorus and nitrogen (Fig. 2A and B). Greater than 94% P removal was achieved, reaching concentrations as low as 0.06 mg L^{-1} effluent P, while the nitrate-nitrogen effluent concentration was less than 6.2 mg L^{-1} and total effluent nitrogen (ammonia + nitrate) was less than 6.6 mg L^{-1}. In addition, the influent VFA-to-phosphorus ratio (Table 2), was also consistent with that observed and/or predicted for successful EBPR (Filipe et al., 2001b; Horgan et al., 2010; Smolders et al., 1994a). However, in contrast to that observed in Reactor A, only 27% of the nitrate synthesized aerobically was reduced during the post-anoxic period (Fig. 2B), and the post-anoxic SDNR, measured at 0.53 mg NO_3 (hr-g MLVSS)$^{-1}$, was less than that exhibited by the mixed microbial consortium in Reactor A (Table 3). Conversely, the anaerobic SDNR was measured at 9.5 mg NO_3 (hr-g MLVSS)$^{-1}$, and more nitrate was reduced anaerobically in Reactor B than observed in Reactor A (Table 3). In fact, process stability in Reactor B was arguably maintained due to the enhanced anaerobic nitrate reduction. While the Reactor A anaerobic denitrification stoichiometry in the later cycles monitored (i.e., 10.24 and 10.29; Table 3) appears similar to that observed in Reactor B, inspection of the entire cycle reveals that (i) significantly more nitrate was removed post-anoxically in Reactor A on 10.24 and 10.29, as contrasted with Reactor B, and (ii) the post-anoxic SDNR was significantly higher for the 10.24 and 10.29 Reactor A measurements as contrasted with Reactor B. Closer inspection of all the Reactor A cycles reveals that total required nitrate removal increased substantially between the 9.8 and 9.11 cycles to the later cycles (approximately 15–35%), and the consortium responded accordingly (although more nitrate bled through to the subsequent anaerobic period). Total required nitrate removal in Reactor B was comparable to 9.11 Reactor A cycle, and the associated Reactor B anaerobic kinetics and stoichiometry were significantly different (Table 3). Thus, it appears that the environmental conditions imposed in Reactor B did not enrich for a consortium as efficient in post-anoxic denitrification.

Contrasted with Reactor A, the Reactor B consortium synthesized approximately half the PHA anaerobically, which led to substantially less aerobic PHA oxidation (Table 4). Also, approximately 20% PHA was carried over to and oxidized post-anoxically, which did not occur with the longer aerobic period in Reactor A. It could be suggested that the reduced PHA synthesis was associated with lower influent VFAs (Figs. 1A vs. 2A), although on a VSS basis the consortium received the same amount of food as Reactor A (Table 2). Thus, the reduced anaerobic PHA synthesis is more likely attributed to increased VFA oxidation anaerobically associated with nitrate reduction, and thus fewer VFAs available for PHA synthesis. One commonality between Reactor A and B was that complete PHA oxidation occurred over a 2.5 h period (Figs. 1C and 2C), regardless of the respiratory environment (aerobic or post-anoxic).

Regarding glycogen synthesis and utilization, amounts comparable to Reactor A were oxidized or synthesized over a full cycle (Table 4). However, as shown (Fig. 2C), glycogen utilization did not commence until approximately one hour into the post-anoxic phase, following depletion of PHA reserves. These results are consistent with those observed by Brdjanovic et al. (1998), who

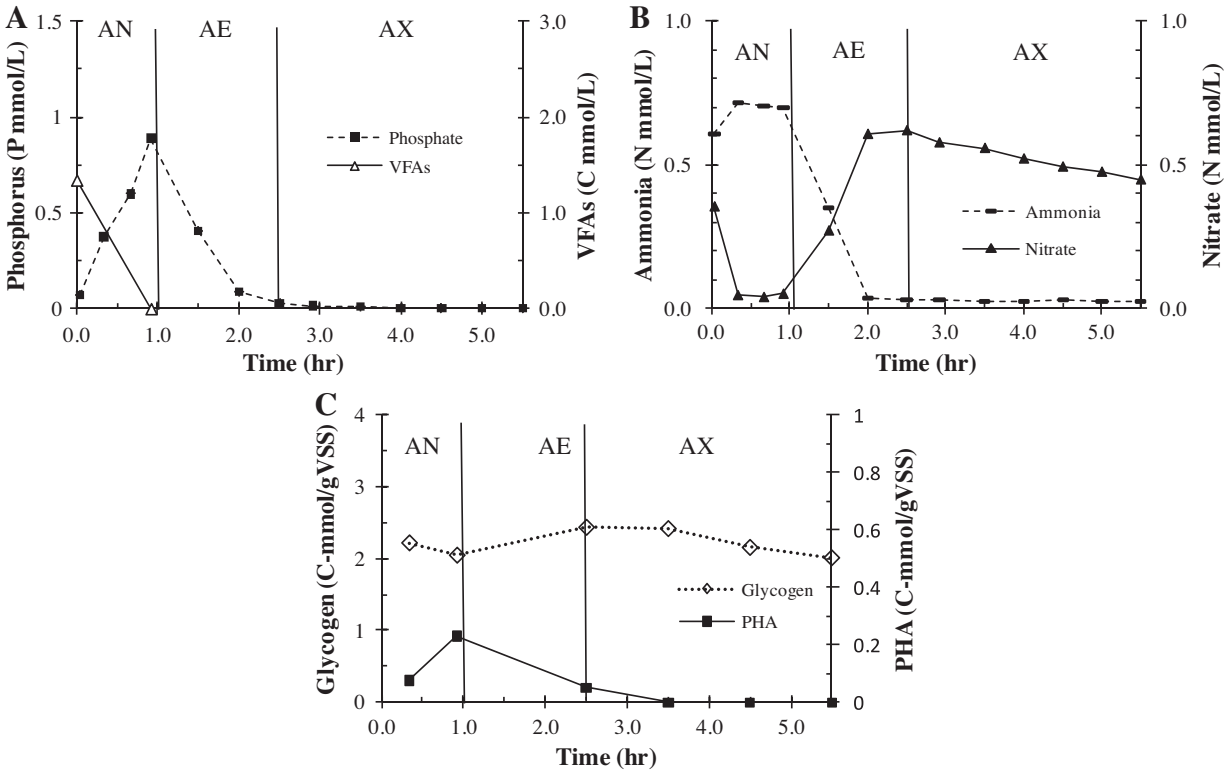

Fig. 2. Performance summary from steady state enhanced biological phosphorus removal reactor (reactor B) operated as a sequencing batch reactor and in post-anoxic mode. Reactor B was operated at a solids retention time of 20 days and a hydraulic residence time of 18 h. Contrasted with reactor A, the aerobic period was shortened by 1 h and the post-anoxic period was lengthened by 1 h. (A) Phosphorus and VFAs profiles in reactor B. (B) Ammonia-N and Nitrate-N profiles in reactor B. (C) Glycogen and PHA profiles in reactor B.

Table 4
Details on carbon stoichiometry during the pre-anoxic/anaerobic, aerobic, and post-anoxic periods for reactors A and B.

Reactor operational period	Parameter	Units	Reactor A		Reactor B
			10.24	10.29	
Pre-anoxic/anaerobic	PHA synthesized	C mmol PHA	1.44	1.08	0.41
		C mmol/g VSS	0.47	0.43	0.23
		mg/g VSS	7.6	5.9	3.3
	VFAs converted to PHA[a]	C mmol VFAs	1.18	0.89	0.34
		C mmol VFA/C mmol PHA	0.82	0.82	0.82
	Glycogen oxidized[c]	C mmol Gly/C mmol VFA	0.54	0.71	0.90
		C mmol Gly/g VSS	0.21	0.25	0.17
		C mmol Gly/C mmol PHA	0.44	0.58	0.74
	VFAs oxidized by NO_3[b]	C mmol VFAs	0.97	2.32	1.26
		C mmol/g VSS	0.32	0.92	0.70
Aerobic	Glycogen synthesized (aerobically)	C mmol/g VSS	0.30	0.67	0.38
	PHA oxidized (aerobically)	C mmol/g VSS	0.45	0.42	0.18
	Glycogen synthesized:PHA oxidized (aerobically)	C mmol/C mmol	0.68	1.58	2.13
Post-anoxic	Glycogen oxidized (post-anoxically)	C mmol/g VSS	0.42	0.55	0.42
	PHA oxidized (post-anoxically)	C mmol/g VSS	0.00	0.00	0.05

[a] Assumes 1.22 C mmol PHA per C mmol VFA.
[b] (Total VFA consumed)–(VFAs converted to PHA).
[c] C mmol Gly/C mmol VFA ratio includes only that fraction of VFAs estimated for PHA synthesis, and excludes VFAs estimated to reduce nitrate.

showed that upon depletion of PHA reserves glycogen is used by DNPAOs for microbial maintenance purposes. The extended post-anoxic period also did not yield significant additional glycogen utilization, as contrasted with the consortium in Reactor A. This response may be associated with the consortium's inability to fully utilize its stored glycogen reserves, which is consistent with observations of Lopez et al. (2006), and Lu et al. (2007), who collectively observed that complete depletion of glycogen pools does not occur even during starvation tests that last days.

Similar to that observed in Reactor A, with a P:C ratio of 0.61 (Table 2), the microbial consortium would appear to have been enriched with PAOs (Lopez-Vazquez et al., 2007; Oehmen et al., 2007). The use of PHA and glycogen post-anoxically also suggests that the consortium was again enriched with DNPAOs. However, the enhanced anaerobic nitrate reduction suggests also that a certain fraction of ordinary heterotrophic organisms (OHOs) were also present; the SDNRs also indicate that the fraction of OHOs was higher than in Reactor A. With the anoxic period increased by 1 h we had expected to observe enhanced post-anoxic denitrification, as contrasted with Reactor A. The presence of OHOs may well have adversely affected post-anoxic denitrification, in that fewer DNPAOs would have been present. However, the reduced intracellular carbon cycling patterns may also have affected the post-anoxic denitrification. Nevertheless, the results showed that process stability can be maintained with a shortened aerobic period and extended anoxic period. These results further demonstrate that post-anoxic denitrification can be driven by either PHA or glycogen.

3.3. Importance of VFA augmentation

EPBR theory specifies that VFAs are metabolized to PHA anaerobically, with necessary reducing equivalents in part derived from glycogen degradation (Smolders et al., 1994a). Liu et al. (1994) conclusively demonstrated the interdependence between PHA and glycogen in EBPR systems. Glycogen is a branched polyglucose carbon storage reserve that is synthesized via gluconeogenesis (Preiss et al., 1983) and degraded via glycolysis (thereby providing reducing equivalents). In regard to synthesis of these polymers, Reactors A and B were augmented with 10% fermenter liquor (v/v), and thus produced sufficient quantities of both PHA and glycogen (Table 4). Further, the carbon and phosphorus cycling patterns were consistent with enriched PAO cultures. To develop a better understanding on the effects of VFA augmentation on process success, we assessed two augmentation extremes: no VFA augmentation, and excess VFA augmentation.

To assess the potential impact of no VFA augmentation on post-anoxic EBPR, a third SBR (identified as Reactor C) was established with the same cycling parameters as Reactor A but without the addition of VFA-rich fermenter liquor. For the first 6 days of operation Reactor C was fed the same wastewater mixture as Reactor A to enrich for a consortium capable of performing post-anoxic denitrification. Thereafter, the consortium was fed exclusively raw wastewater. As shown (Fig. 3A), when the consortium was fed wastewater augmented with VFAs, phosphorus and nitrate cycling patterns were comparable to that observed in Reactors A and B. However, during the subsequent acclimatization period (length of two SRTs), nutrient removal capabilities rapidly deteriorated, ultimately resulting in process failure (Fig. 3B). The consortium stopped denitrifying during the intended post-anoxic period. The resulting nitrate carryover into the subsequent cycle's anaerobic period, and associated use of carbon, prevented the consortium from synthesizing PHA (i.e., in effect the anaerobic period became fully pre-anoxic). The central cause of this process failure was most likely associated with limited anaerobic PHA storage, which caused a lack of glycogen production aerobically. The loss of PHA synthesis can be attributed to insufficient VFAs in the influent and nitrate breakthrough. The F:M ratio in Reactor C was markedly lower than that observed in Reactors A and B (Table 2); moreover, the low influent VFA:P ratio corresponded to a level wherein EBPR could fail (Horgan et al., 2010), and the P:C ratio would suggest negligible PAOs (Lopez-Vazquez et al., 2007; Oehmen et al., 2007).

Not only did the lack of VFA augmentation adversely affect the process, in comparing Reactor C results with that of Reactors A and B, it was also observed that NH_3-N was an important parameter (or more specifically the VFA:NH_3-N ratio; calculated as mg COD:mg NH_3-N). Specifically, if excess NH_4 was present in the influent wastewater or if VFA concentrations were too low (either situation leading to a low VFA:NH_3-N ratio), while nitrification would still readily occur aerobically, incomplete post-anoxic denitrification would be expected due to inadequate carbon. Excess nitrate would then carry over to the subsequent anaerobic cycle and compromise the anaerobic metabolisms. For Reactor C, the VFA:NH_3-N ratio was 3.16 (Table 2). Similarly, in Reactor A a temporary process upset occurred when the ratio fell below 3.33 (data not shown). However, when Reactors A and B were performing optimally, the

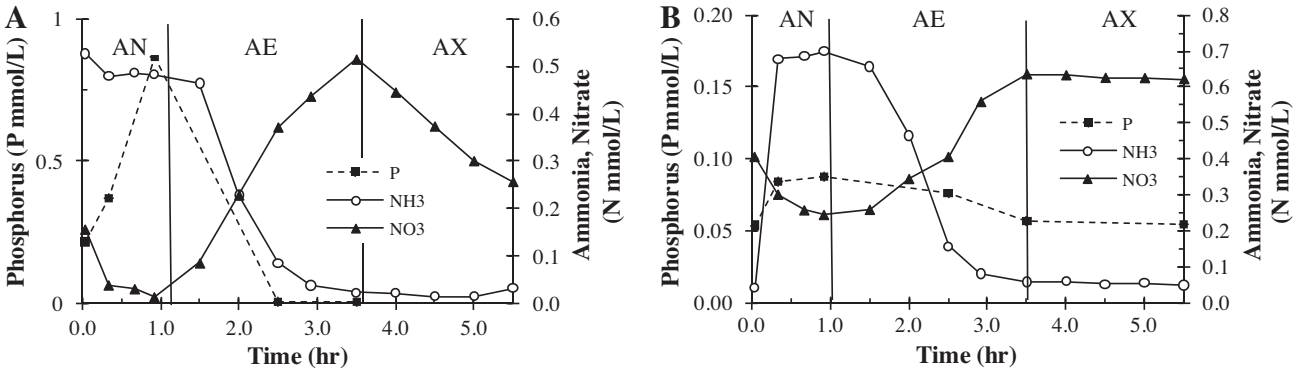

Fig. 3. Performance summary from steady state enhanced biological phosphorus removal reactor (reactor C) operated as a sequencing batch reactor and in post-anoxic mode. Reactor C was operated at a solids retention time of 20 days and a hydraulic residence time of 18 h. The reactor initially operated with a substrate of 90% raw wastewater and 10% fermenter liquor (v:v) to enrich for a consortium capable of phosphorus removal. Operations were then shifted, with the reactor receiving 100% wastewater. Reactor C was operated under the same anaerobic–aerobic–anoxic cycle times as reactor A. (A) Phosphorus, Ammonia-N, and Nitrate-N profiles in reactor C when the wastewater feed composition was 90% raw wastewater and 10% fermenter liquor. (B) Phosphorus, Ammonia-N, and Nitrate-N profiles in reactor C when the wastewater feed composition was 100% raw wastewater (without the addition VFA-rich fermenter liquor).

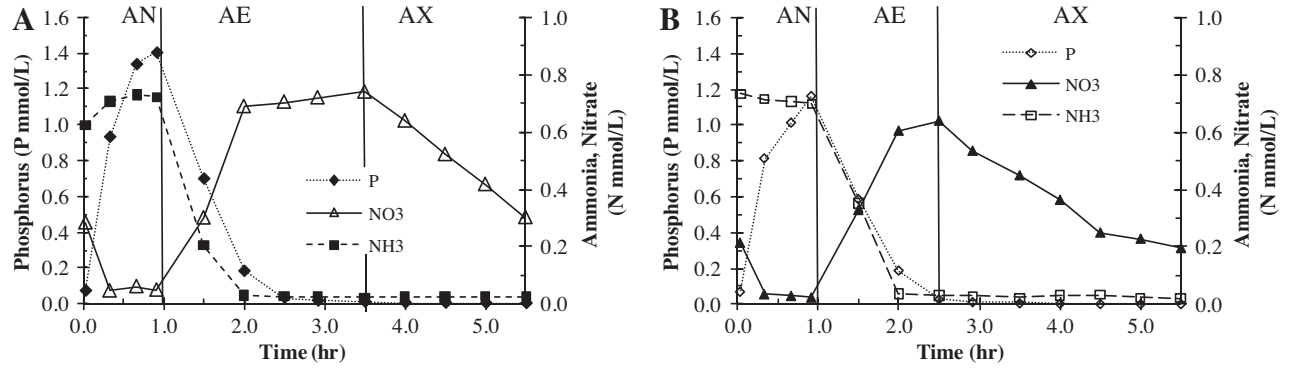

Fig. 4. Performance summary from steady state enhanced biological phosphorus removal reactor (reactor D) operated as a sequencing batch reactor and in post-anoxic mode. Reactor D was operated at a solids retention time of 20 days and a hydraulic residence time of 18 h, and under the same anaerobic–aerobic–anoxic cycle times as reactor A. (A) Phosphorus, Ammonia-N, and Nitrate-N profiles in reactor D when the wastewater feed composition was 90% raw wastewater, 10% fermenter liquor, and further augmented with acetate and propionate. (B) Phosphorus and Nitrate-N profiles in batch run D-1. Biomass was recovered from reactor D at the end of the anaerobic period and then subject to a 1.5 h aerobic period followed by a 3 h post-anoxic period to assess the impact on nitrate removal under variable aerobic–anoxic cycle times (as contrasted with reactor B).

VFA:NH_3-N ratio exceeded 4.1. These observations are consistent with Zhao et al. (2008).

To conversely assess the impact of increased VFAs and to further elucidate the effects of the VFA:NH_3-N ratio on process performance, a new reactor (D; operated for 80 days) was fed the same mixture and operated on the same cycles as Reactor A, but augmented with acetic and propionic acid (150 and 50 mg L^{-1}, respectively). Phosphorus and nitrogen cycling patterns were consistent with those observed in the other VFA augmented systems (Fig. 4A). The effluent P concentration was comparable to that observed in Reactors A and B (0.09 mg P L^{-1}), while the observed post-anoxic SDNR (Table 3) was the highest across all tested reactors (1.36 mg NO_3 (hr-g MLVSS)$^{-1}$). This resulted an effluent ammonia + nitrate concentration <5.0 mg L^{-1}. The amount of glycogen produced aerobically (0.85 C-mmol (g VSS)$^{-1}$) was markedly higher than observed in Reactor A or B. The increased glycogen reserves led to approximately 60% reduction in nitrate post-anoxically, compared with 34% anaerobically. The P:C ratio (Table 2) was again such that PAOs would be predominant (Lopez-Vazquez et al., 2007; Oehmen et al., 2007), and the carbon augmentation yielded a minimum VFA:NH_3-N ratio of over 14 (Table 2), well above that expected for good EBPR performance.

3.4. Toward process optimization

Based on the performance of Reactors A–C, what appeared to be a common link across all reactors associated with post-anoxic denitrification was glycogen. As intracellular glycogen concentrations at the beginning of the post-anoxic period decreased, post-anoxic denitrification performance reduced. To further elucidate the effects of glycogen reserves on post-anoxic denitrification, a batch test using Reactor D biomass was performed (referred to as batch run D-1). Given the elevated glycogen concentration, the purpose of this test was to evaluate if dynamically (for a single cycle) decreasing the aerobic period and increasing the anoxic period would result in improved performance. Biomass was recovered from at the end of the anaerobic period; similar to Reactor B operations, the consortium was then subjected to a 1.5 h aerobic period followed by a 3 h anoxic period. As shown (Fig. 4B), phosphorus and nitrogen cycling patterns were consistent with the parent reactor. The post-anoxic SDNR, estimated at 1.16 mg NO_3 (hr-g MLVSS)$^{-1}$, was effectively the same as that of the parent reactor (Fig. 4A) and was similarly sustained for the first two hours of the post-anoxic period. However, the SDNR decreased in the last hour of the post-anoxic period to approximately 0.32 mg

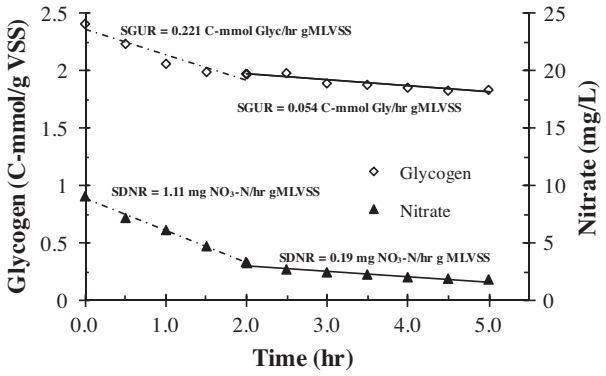

Fig. 5. Glycogen and Nitrate-N profiles in batch run D-2. Biomass was removed from reactor D at the end of the aerobic period and exposed to an extended (5 h) post-anoxic period. SGUR = specific glycogen utilization rate, SDNR = specific denitrification rate.

NO_3 (hr-g MLVSS)$^{-1}$. In contrast to that observed in Reactor B (operated at steady state with the same aerobic and post-anoxic periods as reactor D-1), there were two distinct SDNRs; the maximum SDNR was also approximately twice that observed in Reactor B.

In a second batch experiment, glycogen-rich biomass was obtained from Reactor D at the end of the aerobic period and exposed to an extended (5 h) anoxic period (referred to as batch run D-2). As can be observed (Fig. 5), rapid glycogen utilization again occurred over the first 2 h (a pattern resonating across all tested reactors), concurrent with the rapid depletion of nitrate. At 2 h (coinciding with the end of the anoxic period for the parent Reactor D), the specific glycogen utilization rate (SGUR) decreased rapidly (ultimately by approximately 75%; Fig. 5), with a near order-of-magnitude reduction in the SDNR (from 1.11 to 0.19 mg NO_3 (hr-g MLVSS)$^{-1}$). The shift in SGUR occurred at the same time as observed in parent Reactor D and batch Reactor D-1. The SDNR for the last three hours was less than that observed in Reactor D-1, and the final effluent nitrate concentration was 1.83 mg/L, the lowest obtained in this study. These SGUR results would appear to further support observations of Lopez et al. (2006) and Lu et al. (2007), who collectively observed that complete microbial depletion of glycogen pools may not be possible.

4. Conclusions

The research herein focused on post-anoxic denitrification integrated within enhanced biological phosphorus removal (EBPR). Major findings are as follows:

1. Post-anoxic denitrification in EBPR is predominantly driven by glycogen, although PHA can be used as an electron donor.
2. Glycogen can be significantly depleted post-anoxically without compromising EBPR.
3. Process success requires sufficient VFAs such that anaerobic PHA synthesis and aerobic glycogen synthesis.
4. Sufficient VFAs must be provided such that residual nitrate from the post-anoxic period can be reduced.
5. Dynamically varying aerobic and anoxic contact times could improve nitrogen removal by increasing the amount of glycogen utilized post-anoxically.

Acknowledgements

This material is based upon work supported by the National Science Foundation under Grant No. 0607329. Any opinions, findings, and conclusions or recommendations expressed in this material are those of the authors and do not necessarily reflect the views of the funding agency.

References

Arun, V., Mino, T., Matsuo, T., 1988. Biological mechanism of acetate uptake mediated by carbohydrate consumption in excess phosphorus removal systems. Water Res. 22, 565–570.
Barnard, J. L., Fothergill, S., Secondary phosphorus release in biological phosphorus removal systems, In: WEFTEC, 1998, Orlando, FL, USA.
Braunegg, G., Sonnleitner, B., Lafferty, R.M., 1978. A rapid gas chromatographic method for the determination of poly-β-hydroxybutyric acid in microbial biomass. Eur. J. Appl. Microbiol. 6, 29–37.
Brdjanovic, D., Slamet, A., van Loosdrecht, M.C.M., Hooijmans, C.M., Alaerts, G.J., Heijnen, J.J., 1998. Impact of excessive aeration on biological phosphorus removal from wastewater. Water Res. 32, 200–208.
Carvalho, G., Lemos, P.C., Oehmen, A., Reis, M.A.M., 2007. Denitrifying phosphorus removal: linking the process performance with the microbial community structure. Water Res. 41, 4383–4396.
Clesceri LS, G.A., Eaton, A.D., 1998. Standard Methods for Examination of Water and Wastewater, 20th ed. American Public Health Association, Washington DC.
Filipe, C.D.M., Daigger, G.T., Grady, C.P.L., 2001a. A metabolic model for acetate uptake under anaerobic conditions by glycogen accumulating organisms: stoichiometry, kinetics, and the effect of pH. Biotechnol. Bioeng. 76, 17–31.
Filipe, C.D.M., Daigger, G.T., Grady, C.P.L., 2001b. Stoichiometry and kinetics of acetate uptake under anaerobic conditions by an enriched culture of phosphorus-accumulating organisms at different pHs. Biotechnol. Bioeng. 76, 32–43.
Fuhs, G.W., Chen, M., 1975. Microbiological basis of phosphate removal in the activated sludge process for the treatment of wastewater. Microb. Ecol. 2, 119–138.
Grady Jr., C.P.L., Daigger, G.T., Lim, H.C., 1999. Biological Wastewater Treatment, 2nd ed. Marcel Dekker Inc.
Henze, M., Gujer, W., Mino, T., Matsuo, T., Wentzel, M.C., Marais, G.v.R., 1999. Activated sludge model No. 2d. Water Sci. Technol. 39, 165–182.
Hesselmann, R.P.X., Von Rummell, R., Resnick, S.M., Hany, R., Zehnder, A.J.B., 2000. Anaerobic metabolism of bacteria performing enhanced biological phosphate removal. Water Res. 34, 3487–3494.
Horgan, C.J., Coats, E.R., Loge, F.J., 2010. Assessing the effects of solids residence time and volatile fatty acid augmentation on biological phosphorus removal using real wastewater. Water Environ. Res. 82, 216–226.
Kuba, T., van Loosdrecht, M.C.M., Heijnen, J.J., 1996. Phosphorus and nitrogen removal with minimal COD requirement by integration of denitrifying dephosphatation and nitrification in a two-sludge system. Water Res. 30, 1702–1710.
Kujawa, K., Klapwijk, B., 1999. A method to estimate denitrification potential for predenitrification systems using NUR batch test. Water Res. 33, 2291–2300.
Lemos, P.C., Serafim, L.S., Santos, M.M., Reis, M.A., Santos, H., 2003. Metabolic pathway for propionate utilization by phosphorus-accumulating organisms in activated sludge: 13C labeling and in vivo nuclear magnetic resonance. Appl. Environ. Microbiol. 69, 241–251.
Liu, W.-T., Mino, T., Nakamura, K., Matsuo, T., 1994. Role of glycogen in acetate uptake and polyhydroxyalkanoate synthesis in anaerobic-aerobic activated sludge with a minimized polyphosphate content. J. Ferment. Bioeng. 77, 535–540.
Lopez, C., Pons, M.N., Morgenroth, E., 2006. Endogenous processes during long-term starvation in activated sludge performing enhanced biological phosphorus removal. Water Res. 40, 1519–1530.
Lopez-Vazquez, C.M., Hooijmans, C.M., Brdjanovic, D., Gijzen, H.J., van Loosdrecht, M.C.M., 2007. A practical method for quantification of phosphorus- and glycogen-accumulating organism populations in activated sludge systems. Water Environ. Res. 79, 2487–2498.
Lu, H., Keller, J., Yuan, Z., 2007. Endogenous metabolism of *Candidatus Accumulibacter phosphatis* under various starvation conditions. Water Res. 41, 4646–4656.
Maurer, M., Gujer, W., Hany, R., Bachmann, S., 1997. Intracellular carbon flow in phosphorus accumulating organisms from activated sludge systems. Water Res. 31, 907–917.
Neethling, J. B., Bakke, B., Benisch, M., Gu, A., Stephens, H., Stensel, H. D., Moore, R. "Factors Influencing the Reliability of Enhanced Biological Phosphorus Removal," Water Environment Research Foundation, 2005.
Oehmen, A., Lemos, P.C., Carvalho, G., Yuan, Z.G., Keller, J., Blackall, L.L., Reis, M.A.M., 2007. Advances in enhanced biological phosphorus removal: from micro to macro scale. Water Res. 41, 2271–2300.
Parrou, J.L., Francois, J., 1997. A simplified procedure for a rapid and reliable assay of both glycogen and trehalose in whole yeast cells. Anal. Biochem. 248, 186–188.
Pereira, H., Lemos, P.C., Reis, M.A.M., Crespo, J., Carrondo, M.J.T., Santos, H., 1996. Model for carbon metabolism in biological phosphorus removal processes based on in vivo C-13-NMR labelling experiments. Water Res. 30, 2128–2138.
Preiss, J., Yung, S.-G., Baecker, P.A., 1983. Regulation of bacterial glycogen synthesis. Mol. Cell. Biochem. 57, 61–80.
Qin, L., Liu, Y., Tay, J.-H., 2005. Denitrification on poly-β-hydroxybutyrate in microbial granular sludge sequencing batch reactor. Water Res. 39, 1503–1510.

Satoh, H., Mino, T., Matsuo, T., 1992. Uptake of organic substrates and accumulation of polyhydroxyalkanoates linked with glycolysis of intracellular carbohydrates under anaerobic conditions in the biological excess phosphate removal processes. Water Sci. Technol. 26, 933–942.

Smolders, G.J.F., van der Meij, J., van Loosdrecht, M.C.M., 1994a. Model of the anaerobic metabolism of the biological phosphorus removal process: stoichiometry and pH influence. Biotechnol. Bioeng. 43, 461–470.

Smolders, G.J.F., Vandermeij, J., Vanloosdrecht, M.C.M., Heijnen, J.J., 1994b. Stoichiometric model of the aerobic metabolism of the biological phosphorus removal process. Biotechnol. Bioeng. 44, 837–848.

Tchobanoglous, G., Burton, F.L., Stensel, H.D., 2003. Wastewater engineering: treatment and reuse, 4th ed. McGraw Hill.

Third, K.A., Burnett, N., Cord-Ruwisch, R., 2003. Simultaneous nitrification and denitrification using stored substrate (phb) as the electron donor in an SBR. Biotechnol. Bioeng. 83, 706–720.

Vocks, M., Adam, C., Lesjean, B., Gnirss, R., Kraume, M., 2005. Enhanced post-denitrification without addition of an external carbon source in membrane bioreactors. Water Res. 39, 3360–3368.

Zhang, C.Y., Yinguang, C., Randall, A.A., Guowei, G., 2008. Anaerobic metabolic models for phosphorus- and glycogen-accumulating organisms with mixed acetic and propionic acids as carbon sources. Water Res. 42, 3745–3756.

Zhao, C.H., Peng, Y.Z., Wang, S.Y., Takigawa, A., 2008. Effects of influent C/N ratio, C/P ratio and volumetric exchange ratio on biological phosphorus removal in UniFed SBR process. J. Chem. Technol. Biotechnol. 83, 1587–1595.